polymers

MDPI

Article

Effects of Repulsion Parameter and Chain Length of Homopolymers on Interfacial Properties of $A_n/A_{x/2}B_xA_{x/2}/B_m$ Blends: A DPD Simulation Study

Dongmei Liu [1], Kai Gong [1], Ye Lin [1], Huifeng Bo [1,*], Tao Liu [1,*] and Xiaozheng Duan [2,3,*]

[1] School of Science, North China University of Science and Technology, Tangshan 063210, China; dmliu@ncst.edu.cn (D.L.); gongkai0524@163.com (K.G.); linye315317@163.com (Y.L.)
[2] State Key Laboratory of Polymer Physics and Chemistry, Changchun Institute of Applied Chemistry, Chinese Academy of Sciences, Changchun 130022, China
[3] State Key Laboratory of Molecular Engineering of Polymers, Department of Macromolecular Science, Fudan University, Shanghai 200438, China
* Correspondence: bohuifeng@ncst.edu.cn (H.B.); liutao@ncst.edu.cn (T.L.); xzduan@ciac.ac.cn (X.D.); Tel.: +86-315-8805860 (H.B. & T.L.); +86-431-85262479 (X.D.)

Abstract: We explored the effects of the repulsion parameter (a_{AB}) and chain length (N_{HA} or N_{HB}) of homopolymers on the interfacial properties of $A_n/A_{x/2}B_xA_{x/2}/B_m$ ternary polymeric blends using dissipative particle dynamics (DPD) simulations. Our simulations show that: (i) The ternary blends exhibit the significant segregation at the repulsion parameter (a_{AB} = 40). (ii) Both the interfacial tension and the density of triblock copolymer at the center of the interface increase to a plateau with increasing the homopolymer chain length, which indicates that the triblock copolymers with shorter chain length exhibit better performance as the compatibilizers for stabilizing the blends. (iii) For the case of N_{HA} = 4 (chain length of homopolymers A_n) and N_{HB} (chain length of homopolymers B_m) ranging from 16 to 64, the blends exhibit larger interfacial widths with a weakened correlation between bead A_n and B_m of homopolymers, which indicates that the triblock copolymer compatibilizers ($A_{x/2}B_xA_{x/2}$) show better performance in reducing the interfacial tension. The effectiveness of triblock copolymer compatibilizers is, thus, controlled by the regulation of repulsion parameters and the homopolymer chain length. This work raises important considerations concerning the use of the triblock copolymer as compatibilizers in the immiscible homopolymer blend systems.

Keywords: dissipative particle dynamics; interfacial property; compatibilizer

Citation: Liu, D.; Gong, K.; Lin, Y.; Bo, H.; Liu, T.; Duan, X. Effects of Repulsion Parameter and Chain Length of Homopolymers on Interfacial Properties of $A_n/A_{x/2}B_xA_{x/2}/B_m$ Blends: A DPD Simulation Study. *Polymers* **2021**, *13*, 2333. https://doi.org/10.3390/polym13142333

Academic Editors: Zaixing Jiang, Shuai Zhang, Dawei Zhang, Guo-Lin Gao and Sergio Torres-Giner

Received: 11 June 2021
Accepted: 13 July 2021
Published: 16 July 2021

1. Introduction

Improving the performance of polymer materials in scientific and industrial applications can be achieved by mixing different components with complementary properties [1,2]. Typically, the mixing of two (or more) thermodynamically immiscible homopolymers (components) results in unstable interfaces within the systems and the poor mechanical properties of the blends [3]. For optimization, amphiphilic copolymers are often used as compatibilizers to improve the interfacial stability of highly immiscible mixtures in multi-constituent polymeric systems [4]. Specifically, the interfacially active amphiphilic copolymers preferentially aggregate at the interfaces between phase-separated homopolymers, which leads to a significant reduction in the interfacial tension between the two phases [5,6]. In consequence, the interfacial adhesion and mechanical properties of the blends can be improved by the significant increase in the thickness of the interface between the two phases during the mixing process [7–9].

In the past decades, considerable attention has been focused on the interfaces of binary and ternary blends [10–29]. For example, Qian et al. investigated the interfacial properties of the A_n/B_m binary homopolymers blends using DPD simulation [8]. It is found that when the chain length of the homopolymers was fixed, the interfacial tension

increases with increasing Flory–Huggins interaction parameter; however, when the Flory–Huggins interaction parameter and the chain length of one homopolymer component were fixed, the interfacial tension increases slightly with increasing another homopolymer chain length. Guo et al. also employed DPD simulation to investigate the interfacial properties of $A_2/A_2B_8/B_2$ and $A_2/A_2B_8/B_{10}$ ternary mixtures [1]. They found that swelling is responsible for the stretching and orienting of the diblock copolymers chains and the reduced interfacial density of copolymers. The pioneering systematic experimental studies of homopolymer/triblock copolymer/homopolymer blend systems were performed by T. P. Russell et al. and E. J. Kramer et al. [22,23]. They initially reported that the triblock copolymers could serve as better compatibilizers than the diblock copolymers due to their higher critical micelle concentration for the same copolymer composition and concentration. Wolf et al. [24] investigated the poly(dimethyl siloxane)/poly(dimethyl siloxane)-poly(ethylene oxide)-poly(dimethyl siloxane) (PDMS/PDMS-PEO-PDMS/PEO) ternary blends. It was found that the interfacial tension increases with the rising of the temperature. Subsequently, through comparing the effects of the PDMS-PEO diblock copolymer compatibilizers and the PDMS-PEO-PDMS triblock copolymer compatibilizers on the interfacial tension of the PDMS/PEO blends, it was concluded that the interfacial tension of the blends mainly depended on the length of PDMS block, and has little correlation with the length of the PEO blocks and the compatibilizer architecture [25]. Xu et al. investigated the effects of Polymethyl methacrylate-polyethylene-Polymethyl methacrylate (PMMA-PE-PMMA) triblock copolymers on the properties of PE/PMMA blends. Their experiments showed that the PMMA-PE-PMMA triblock copolymers can significantly enhance the elastic modulus, the hardness, and the stability of the blends [26]. Sun et al. studied Poly(lactic acid)/poly(lactic acid)-poly(butylene adipate-*co*-terephthalate)poly(lactic acid)/poly(butylene adipate-*co*-terephthalate) (PLA/PLA-PBAT-PLA/PBAT) ternary blends, which showed that the addition of PLA-PBAT-PLA enhanced the miscibility and interfacial bonding strength between PLA/PBAT blends [27]. Recently, the interfacial tension of polypropylene/styrene-ethylene/polystyrene and polypropylene/butylene-styrene/polystyrene blends was investigated by Zhao et al [28], which indicated that the copolymers styrene–ethylene and butylene–styrene with a shorter chain length show higher efficiency than their long-chain length counterparts. In the previous study, we have investigated the dependence of the interfacial properties of symmetric ternary polymeric blends on the chain length and concentration of triblock copolymer, which also indicated that the triblock copolymers with shorter chain length perform a higher efficiency [29].

Despite the progress in the study of structural and thermodynamic properties of the blend systems, there are still many ambiguities in the $A_n/A_{x/2}B_xA_{x/2}/B_m$ ternary blends systems. For example, the study on the effect of repulsion parameters of different kinds of beads and the chain length of homopolymers on the ternary $A_n/A_{x/2}B_xA_{x/2}/B_m$ polymeric blends remains limited. In fact, the interfacial tension and the conformation of the ternary blends also depended on the repulsion parameter between the A and B beads, and on the chain length of homopolymers. It is necessary to clarify the effects of such factors on the structural and interfacial properties of the ternary blends.

In this work, we further use DPD simulation to explore the interfacial properties of symmetric ternary $A_n/A_{x/2}B_xA_{x/2}/B_m$ polymeric blends. We first briefly introduce the theory and algorithm of DPD simulations used in our work. We then systematically analyze the effects of repulsion parameters between beads A and B, and the chain length of the homopolymers on the properties of the interfaces in the blends, such as the interfacial tension, the density distribution of different beads and the detailed chain conformations of the triblock copolymers. Our work indicates that when the repulsion parameter is set to be a_{AB} = 40, the ternary blends are significantly segregated and there exist flat interfaces between the two incompatible homopolymers. The triblock copolymers are more efficient in compatibilizing short incompatible homopolymers. Finally, we briefly summarize our results and offer some concluding remarks.

2. Methods

In a previous study, we employed the DPD method to investigate the effect of the chain length and concentration of triblock copolymer compatibilizers on the interfacial tension between two immiscible homopolymers [29]. The model of this work is constructed based on our previous work and other studies [8,9,29–41]. Herein, we briefly introduce the model; interested readers could refer to these studies for the further development of the model.

2.1. Model

We coarse-grain all the polymers as connected beads. The time evolution of the beads in the simulation satisfies Newton's equations of motion,

$$\frac{d\mathbf{r}_i}{dt} = \mathbf{v}_i;\ m_i\frac{d\mathbf{v}_i}{dt} = \mathbf{f}_i \tag{1}$$

where $\mathbf{r_i}$, $\mathbf{v}_i$ and m_i represent the position, velocity and mass of the *i*-th bead, respectively. The sum of conservative forces, dissipative forces, random forces and harmonic spring forces represents the total force $\mathbf{f}_i$ acting on bead *i*, which can be expressed by the following formula [42]:

$$\mathbf{f}_i = \sum_{j\neq i}\left(\mathbf{F}_{ij}^C + \mathbf{F}_{ij}^D + \mathbf{F}_{ij}^R\right) + \mathbf{F}_i^S \tag{2}$$

The conservative force $\mathbf{F}_{ij}^C$, dissipative force $\mathbf{F}_{ij}^D$ and random force $\mathbf{F}_{ij}^R$ are described as,

$$\mathbf{F}_{ij}^C = -a_{AB}\omega^C(\mathbf{r}_{ij})\mathbf{e}_{ij} \tag{3}$$

$$\mathbf{F}_{ij}^D = -\gamma\omega^D(\mathbf{r}_{ij})(\mathbf{v}_{ij}\cdot\mathbf{e}_{ij})\mathbf{e}_{ij} \tag{4}$$

$$\mathbf{F}_{ij}^R = \sigma\omega^R(\mathbf{r}_{ij})\xi_{ij}\cdot t^{-1/2}\mathbf{e}_{ij} \tag{5}$$

in which the repulsion force parameter a_{AB} is a constant used to describe the repulsion between the different kinds of beads. $\mathbf{r}_{ij} = \mathbf{r}_i - \mathbf{r}_j$, $r_{ij} = |\mathbf{r}_{ij}|$, $\mathbf{e}_{ij} = \mathbf{r}_{ij}/r_{ij}$, and $\mathbf{v}_{ij} = \mathbf{v}_i - \mathbf{v}_j$. γ, σ and ξ_{ij} are interpreted as the friction coefficient, amplitude of the noise and Gaussian random number with zero mean and unit variance, respectively. ω^C, ω^D and ω^R denote the three weight functions for the conservative, dissipative and random forces, respectively. For the conservative force F_{ij}^C, we simply choose $\omega^C(\mathbf{r}_{ij}) = 1 - r_{ij}$ for $r_{ij} < 1$ and $\omega^C(\mathbf{r}_{ij}) = 0$ for $r_{ij} \geq 1$. Unlike $\omega^C(\mathbf{r}_{ij})$, $\omega^D(\mathbf{r}_{ij})$ and $\omega^R(\mathbf{r}_{ij})$ have a certain relation according to the fluctuation–dissipation theorem [31]:

$$\omega^D(r) = \left[\omega^R(r)\right]^2,\ \sigma^2 = 2\gamma k_B T \tag{6}$$

where k_B and T represent the Boltzmann constant and the temperature, respectively. The weight functions of dissipative and random forces are simply chosen as the previous work of Groot and Warren [42]:

$$\omega^D(r) = \left[\omega^R(r)\right]^2 = \begin{cases} (1-r)^2 & (r<1) \\ 0 & (r\geq 1) \end{cases} \tag{7}$$

The harmonic spring force $\mathbf{F}_i^S$ is employed to account for the connection intrachain beads and can be expressed as

$$\mathbf{F}_i^S = \sum_j C\mathbf{r}_{ij} \tag{8}$$

where $C = 4.0$ is the spring constant.

The conservative interaction strength between different types of beads a_{AB} (A and B are unlike beads) is chosen according to the linear relation with Flory–Huggins parameters χ for polymers [42]

$$a_{AB} \approx a_{AA} + 3.50\chi_{AB} \tag{9}$$

In this work, the repulsion parameter between the same type of beads is set as $a_{BB} = a_{AA} = 25$.

2.2. Simulation Details

We use the Materials Studio Program (Accelrys Inc.) to perform DPD simulations in a 30 × 30 × 30 simulation box with three-dimensional periodic boundary conditions. The radius of interaction, the bead mass and the temperature are set as $r_c = k_BT = 1$ in the reduced unit (where r_c is the interaction radius, m is the mass of bead, k_BT is the temperature) according to the defaults of the program. The number density of the beads in the simulation system is fixed as $\rho = 3$, and therefore, there are approximately 81,000 beads in each simulated system. The time step is taken as 0.05, and the friction coefficient γ is chosen as 4.5.

In this study, we focus on the ternary blends $A_n/A_2B_4A_2/B_m$ with the triblock copolymer concentration of c_{cp} = 0.05, 0.2 and the blends $A_n/A_7B_{14}A_7/B_m$ with c_{cp} = 0.2 (c_{cp} is referred as the number density of the triblock copolymer, n and m are the numbers of bead A and B of two immiscible homopolymers).

In order to examine the effects of the repulsion parameters a_{AB} on interfacial properties, we vary a_{AB} from 30 to 75. To investigate the chain length of homopolymers of interfacial properties, we change the chain length of homopolymers from N_H = 3 to 60 for the $A_n/A_2B_4A_2/B_m$ and $A_n/A_7B_{14}A_7/B_m$ (here the chain length of A_n and B_m are the same, hence, we use N_H to denote the chain length of homopolymers, i.e., $N_H = n = m$). In this study, the homopolymers and triblock copolymers are initially placed in the distinct parts in the box along the x-direction. These artificial initial configurations can speed up the formation of the interfaces perpendicular to the x-direction, so as to enhance the computing efficiency [8]. We first perform 2.0 × 10^5 steps, which have proven to be sufficient to ensure that the system reaches an equilibrium state. To confirm the system equilibration, we calculate ${R_g}^2$ and ${R_{ee}}^2$ of copolymers as a function of the simulation time (as illustrated in Figure S1 in the supplementary material). Additionally, our previous work [29] and another previous study [43] also show that the relative systems could reach equilibration during such simulation time. Furthermore, we perform 5 × 10^4 steps in the further production process. As shown in Figure S1 (t > 100,000 steps) in the supplementary material, although the fluctuation effects are not significant in our simulation, we still performed several parallel simulations and obtained final accurate results from the order of 10^3 to 10^4 independent statistical samples.

In a ternary blend with a flat interface, interfacial tension analysis can be used to detect the interface physical properties and stability of the blends. In addition, the interfacial tension results obtained from DPD simulations [33–35] are usually used as basic data to compare with Groot and Warren's theoretical solutions. Here, we calculate the interfacial tension according to the Irving–Kirkwood equation [44]. The result is obtained by integrating the stress difference in the x-direction,

$$\gamma_{DPD} = \int \left[P_{xx} - \frac{1}{2}\left(P_{yy} + P_{zz}\right) \right] dx \tag{10}$$

where P represents the pressure tensor, defined as the stress per unit area, P_{xx} represents the stress perpendicular to the interface and P_{yy} and P_{zz} represent the stress parallel to the interface.

We also calculate the mean-square radii of gyration $<{R_g}^2>$, mean-square end-to-end distance $<{R_{ee}}^2>$ and the chain orientation parameter q of the triblock copolymers to characterize the detailed polymer conformations. We calculate the orientation parameters q according to the work of Qian et al. (Ref. [8]):

$$q = \frac{\left(\left\langle R_g^2 \right\rangle_x - 1/2\left(\left\langle R_g^2 \right\rangle_y + \left\langle R_g^2 \right\rangle_z\right)\right)}{R_g^2} \tag{11}$$

where $<R_g^2>_x$ is the normal component of the mean-square radii of gyration $<R_g^2>$, and $<R_g^2>_y$ and $<R_g^2>_z$ are the transverse components of mean-square radii of gyration $<R_g^2>$.

In addition, we calculate the interfacial width w between the immiscible homopolymers A_n and B_m according to the work of Guo et al. (Ref. [1]), the interfacial width w is obtained by fitting the function $\tanh((x + d)/w)$ to the profile $(\rho^A(x)–\rho^B(x))/\rho(x)$ across the two interfaces, where d is the shift of the interface center along with the x directions.

3. Results and Discussion

3.1. Effect of the Repulsion Parameters a_{AB}

To fundamentally understand how the repulsion parameter influences the interfacial properties of homopolymer/triblock copolymer/homopolymer ternary blends, we fix the chain length of homopolymers $N_H = 8$ and vary the repulsion parameter a_{AB} between beads A and B from 30 to 75 for the triblock copolymer $A_2B_4A_2$ and $A_7B_{14}A_7$ systems. Figures 1 and 2 show the morphology snapshots and density profiles of triblock copolymers for the blend systems of $A_8/A_2B_4A_2/B_8$ and $A_8/A_7B_{14}A_7/B_8$, respectively. We found that most triblock copolymers are segregated at the interface, and the central B beads of the triblock copolymers preferentially segregate into the bulk phase of homopolymers B_8, and both the end A beads segregate into the bulk phase of homopolymers A_8, which indicates that the triblock copolymers form a "hairpin" type of conformation at the interfaces, as illustrated in Figure S2a. The structures of the copolymers result in the reduction of immiscible homopolymer contacts. Figure S2b in the supplementary material shows the morphology snapshot of the copolymer beads in blend $A_8/A_2B_4A_2/B_8$ with $a_{AB} = 30$, which illustrates that most triblock copolymers aggregate at the plane interface, and the rest of the copolymers aggregate into the homopolymer phase, as illustrated in Figure 2. We further consider the blends $A_8/A_2B_4A_2/B_8$ with the triblock copolymer concentration of $c_{cp} = 0.2$. Figure S3 in the supplementary material shows the morphology snapshots of the blend. It can be seen that at such a condition, the interfaces have reached saturation, and the triblock copolymers $A_2B_4A_2$ aggregate in a large amount in homopolymers A_8, which could lead to the inaccurate calculation of the interfacial tension and the interfacial width. Moreover, in our previous work (ref. [29]), we found that the system $A_8/A_7B_{14}A_7/B_8$ with $c_{cp} = 0.05$ exhibits larger interface tension, which indicates the instability of the interfaces. Due to the interface stability at the optimized triblock copolymer concentrations of $c_{cp} = 0.05$ for $A_n/A_2B_4A_2/B_m$ and $c_{cp} = 0.2$ for $A_n/A_7B_{14}A_7/B_m$, we focus on these systems for the detailed analysis.

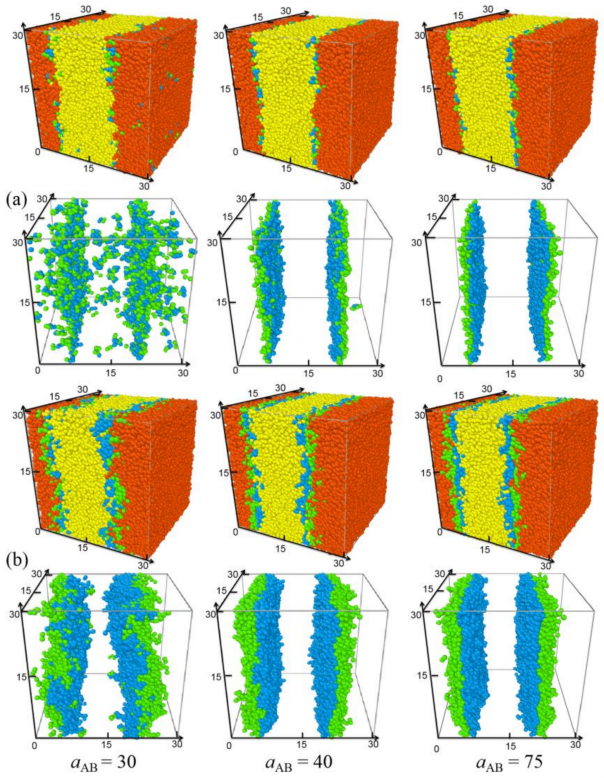

Figure 1. Morphology snapshots for ternary mixtures at different repulsion parameters a_{AB} between A and B beads. The chain lengths and concentrations of the triblock are set as (**a**) $A_2B_4A_2$, $c_{cp} = 0.05$ and (**b**) $A_7B_{14}A_7$, $c_{cp} = 0.2$, respectively. The red and yellow spheres denote bead A and bead B of homopolymers A_8 and B_8, and the green and blue spheres represent beads A and B of the triblock.

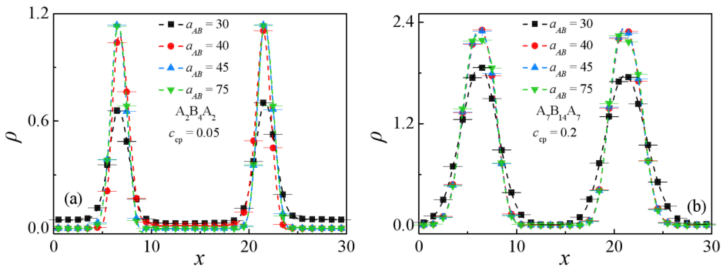

Figure 2. Density profiles of beads A + B of the triblock copolymer along the x-axis as a function of the repulsion parameter a_{AB} with (**a**) $A_2B_4A_2$, $c_{cp} = 0.05$ and (**b**) $A_7B_{14}A_7$, $c_{cp} = 0.2$.

Figures 1 and 2 show that the segregation of the triblock copolymer at the interface strongly depends upon the repulsion parameter a_{AB}. As the repulsion parameter $a_{AB} = 30$, although the system shows an obvious interface and most of the triblock copolymers aggregate near the interface between homopolymer A_8 and B_8, the interface of the blend is not very smooth (see Figure 1a,b with $a_{AB} = 30$) and the copolymers significantly penetrate the homopolymer bulk phase, as shown by the black solid squares in Figure 2a,b. As the repulsion parameter increases from $a_{AB} = 30$ to 40, all of the triblock copolymers aggregate at the interface of the ternary blends (as shown by $a_{AB} = 40$ in Figure 1), resulting in the increase in density of A + B beads of the triblock copolymers at the center of the interface (see the red solid dots in Figure 2a,b). However, as the repulsion parameter further increases from $a_{AB} = 40$ to 75, the morphology and the density of the triblock copolymers change slightly. These findings indicate that as the repulsion parameter is set to be $a_{AB} = 40$, the $A_8/A_2B_4A_2/B_8$ and $A_8/A_7B_{14}A_7/B_8$ ternary blends exhibit significant segregations, i.e.,

the two immiscible homopolymers are completely isolated by the copolymers, and almost all copolymers aggregate at the interface.

In order to quantitatively study the effects of the repulsion parameters a_{AB} on the interfacial properties of the blend's materials, we calculated the interfacial tension γ, the interfacial thickness w, the orientation parameter q, the mean-square radii of gyration $<R_g^2>$ and the mean-square end-to-end distance $<R_{ee}^2>$ at different repulsion parameter a_{AB}, as shown in Figures 3 and 4. Apparently, the interfacial tension γ increases monotonically with increasing the repulsion parameter a_{AB} for the two blend systems, as shown by Figure 3a. This finding is consistent with the simulations of the A_n/B_m binary blends of Qian et al. [8] and the $A_2/A_2B_8/B_2(B_{10})$ ternary blends by Guo et al. [1]. Helfand and Tagami predicted the dependence of the interfacial tension γ on the interaction parameters χ by SCFT for the interface of homopolymer/homopolymer in the limit of infinite chain length, i.e., $\gamma = \rho b k_B T \sqrt{6\chi}$, which indicated that the interfacial tension is proportional to $\sqrt{6\chi}$ [45]. In our simulations, Figure 3a also shows a larger interfacial tension γ of blends at c_{cp} = 0.05. We inferred that the increase of the interfacial tension γ for this case with small copolymer concentration can be attributed to the distribution of copolymers beads, as illustrated in Figure 2a,b. It is shown that at the copolymer concentration c_{cp} = 0.05, the density of the beads A + B of the triblock copolymers exhibits a decrease, which results in the enhanced correlations between beads of immiscible homopolymers. Figure 3b shows the interfacial width w of the $A_8/A_2B_4A_2/B_8$ and $A_8/A_7B_{14}A_7/B_8$ system. For the $A_8/A_2B_4A_2/B_8$ system, as the repulsion parameter increases from a_{AB} = 35 to 55, the interfacial width w decreases, as the a_{AB} increases further to 75, the interfacial width w of the changes slightly. In the $A_8/A_7B_{14}A_7/B_8$ system, as the repulsion parameter increases from a_{AB} = 35 to 75, the interfacial width w decrease first and then increases slowly. We inferred that the interface width w, which decreases first and changes slightly for the two cases with increasing the repulsion parameters a_{AB}, is related to the distribution of copolymers beads, i.e., as the density distribution of A + B beads of the triblock copolymer at the center of the interface is smaller, more A + B beads of the triblock copolymer penetrate the homopolymer phases, and this broader distribution of the triblock copolymer results in a larger interfacial width w.

Figures 3c and 4 show the dependence of the chain orientation parameter q and the dimension (the mean-square radii of gyration $<R_g^2>$ and its three components $<R_g^2>_x$, $<R_g^2>_y$, $<R_g^2>_z$, the mean-square end-to-end distance $<R_{ee}^2>$ and its three components $<R_{ee}^2>_x$, $<R_{ee}^2>_y$, $<R_{ee}^2>_z$ of the copolymer, which can be used to characterize the detailed conformation of the copolymers at the interface) of the triblock copolymer on the repulsion parameter a_{AB}. It can be seen that the triblock chain orientation parameter q increases with increasing repulsion parameter a_{AB}; for the $A_8/A_2B_4A_2/B_8$ system, $q < 0$ (the black solid square in Figure 3c), and for the $A_8/A_7B_{14}A_7/B_8$ system, $q > 0$ (the red solid spheres in Figure 3c). Accordingly, Figure 4a,b show that $<R_g^2>$ and $<R_g^2>_x$ increase with increasing repulsion parameter a_{AB}, implying that the triblock copolymers are more stretched at larger repulsion parameters. In addition, we found that the $<R_g^2>_y$ and $<R_g^2>_z$ of triblock copolymers in y and z directions parallel to the interface are larger than the perpendicular $<R_g^2>_x$ in the x-direction for the $A_8/A_2B_4A_2/B_8$ system (Figure 4a), which is in contrast with the $A_8/A_7B_{14}A_7/B_8$ system (Figure 4b). This finding is in agreement with the q of the two systems. Figure 4c,d show that the x-components $<R_{ee}^2>_x$ of mean-square end-to-end distance decreases with increasing repulsion parameter a_{AB}, and the $<R_{ee}^2>_y$ and $<R_{ee}^2>_z$ are larger than $<R_{ee}^2>_x$. These results indicated that as the repulsion parameter increase a_{AB}, the distribution of the end block A beads of the triblock copolymers is broader (as illustrated in Figure S4a,b) in the supplementary material, thus the x component of $<R_{ee}^2>_x$ of the triblock copolymers is larger.

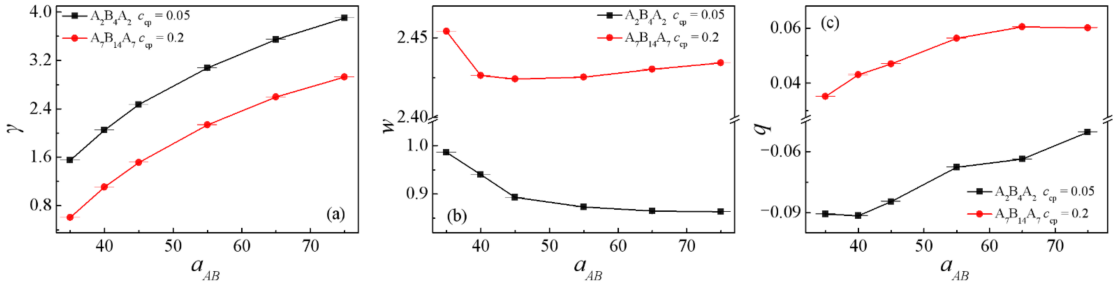

Figure 3. Interfacial tension γ (**a**), interfacial thickness w (**b**) and orientation parameter (**c**) of the triblock as a function of repulsion parameters a_{AB} between beads A and B.

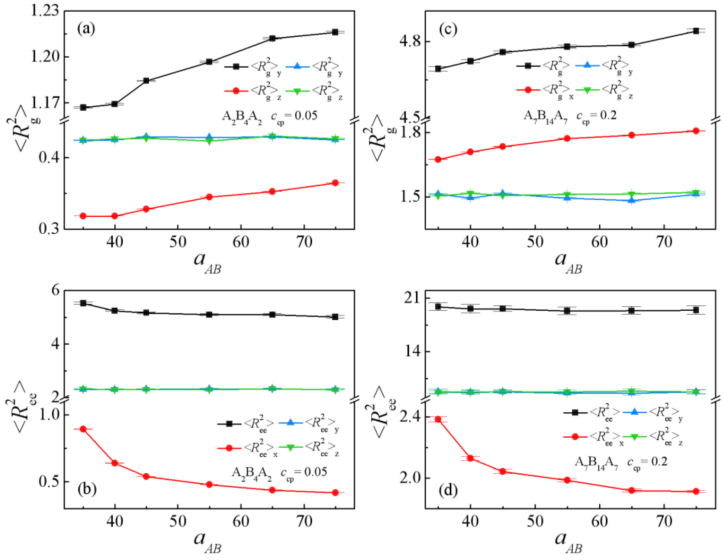

Figure 4. Mean-square radii of gyration $<R_g^2>$ and the three components $<R_g^2>_x$, $<R_g^2>_y$, $<R_g^2>_z$ as a function of the repulsion parameter a_{AB} with (**a**) $A_2B_4A_2$, c_{cp} = 0.05, (**c**) $A_7B_{14}A_7$, c_{cp} = 0.2. Mean-square end-to-end distance $<R_{ee}^2>$ and the three components $<R_{ee}^2>_x$, $<R_{ee}^2>_y$, $<R_{ee}^2>_z$ as a function of the repulsion parameter a_{AB} with (**b**) $A_2B_4A_2$, c_{cp} = 0.05, (**d**) $A_7B_{14}A_7$, c_{cp} = 0.2.

As shown by the previous studies, polymer blends with the greater interfacial tension exhibit the worse stability and adhesion of the interface [2]. Through comprehensive analysis for the interfacial tension γ of the blends, as well as the density distribution, chain orientation parameter q and dimension of the triblock copolymers, we conclude that as the repulsion parameter is a_{AB} = 40, the ternary blends exhibit significant segregation with a lower interfacial tension and stronger adhesion. Therefore, in the following part of the manuscript, we fix the repulsion parameter of different types of beads as a_{AB} = 40, and investigated the effect of chain length of homopolymers on the interfacial properties of $A_n/A_{x/2}B_xA_{x/2}/B_m$ polymeric blends.

3.2. Effect of Chain Length of Homopolymers

3.2.1. Symmetric Homopolymers with $N_{HA} = N_{HB}$

We first consider the cases for homopolymers A_n and B_m with identical chain lengths, i.e., $N_{HA} = N_{HB} = N_H$. Herein, the homopolymer chain length is varied from 3 to 60 for the triblock copolymer $A_2B_4A_2$ and $A_7B_{14}A_7$ ternary blends system. Figure 5 shows the relative density profiles of the triblock copolymers. It is shown that the segregation of the triblock copolymers at the interface depends on the chain length of homopolymers. The density of A + B beads of the triblock copolymer at the center of the interface increases with increasing the homopolymer chain length from N_H = 3 to N_H = 16. As the chain length of

the homopolymer increases from N_H = 16 to N_H = 60, the density of A + B beads of the triblock copolymer at the center of the interface remains almost unchanged.

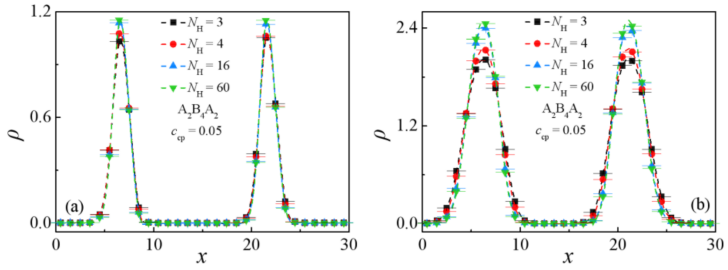

Figure 5. Density profiles of beads A + B of the triblock copolymer along the *x*-axis as a function of the homopolymer chain length with (**a**) $A_2B_4A_2$, c_{cp} = 0.05, (**b**) $A_7B_{14}A_7$, c_{cp} = 0.2.

Figure 6a,b show the dependence of the interfacial tension γ and the interfacial width w on the homopolymers chain length N_H, respectively. The obtained interfacial tension γ rapidly increases and the interfacial width w decreases with increasing the homopolymer chain length from N_H = 3 to 32, whereas as N_H increases from 32 to 60, both the interfacial tension γ and the interfacial width w reach a plateau. These results show that: (i) the ternary blend system with shorter homopolymer chain length exhibits a lower interfacial tension γ, which implies that the triblock copolymers compatibilizers show better performance in reducing the interfacial tension of the ternary blends with shorter homopolymer chain length. This is because that the shorter the chain length of the homopolymers can cause a wider interfacial width w (Figure 6b), which results in the decayed correlations between beads of immiscible homopolymers and the smaller the interfacial tension γ.

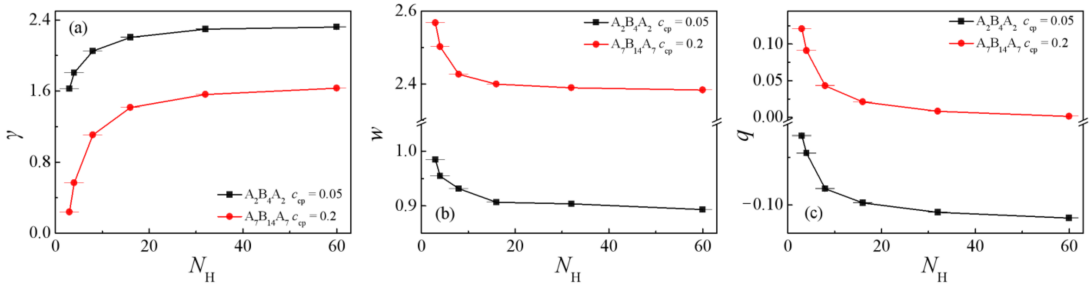

Figure 6. Interfacial tension γ (**a**), interfacial thickness w (**b**), and orientation parameter q of the triblock (**c**) as a function of the homopolymer chain length N_H (N_H = 3, 4, 8, 16, 32, 48, 60).

Figures 6c and 7 show the chain orientation parameter q and the dimension of the triblock copolymers on the homopolymers chain length N_H. We found that as the chain length of homopolymers increase from N_H =3 to 60, the chain orientation parameters q decrease first and then reach a plateau for the two systems (Figure 6c), which indicates that the triblock copolymers are more stretched at shorter homopolymer chain length in the *x*-direction, being perpendicular to the interface. Figure 7a,b show that $<R_g^2>$, $<R_g^2>_x$, and $<R_{ee}^2>_x$ of the copolymers decrease rapidly with the increasing of homopolymer chain length from N_H =3 to 8, whereas as N_H further increases from 8 to 60, only $<R_{ee}^2>_x$ decreases slowly with the $A_2B_4A_2$ system. For the $A_7B_{14}A_7$ system, the $<R_g^2>$, $<R_g^2>_x$ and $<R_{ee}^2>_x$ decrease rapidly with the increase of homopolymer chain length from N_H = 3 to 16, but as N_H increases from 16 to 60, the $<R_g^2>$, $<R_{ee}^2>_x$ and their three components almost unchanged (as illustrated in Figure 7c,d). We also found that as N_H increases, the y and z components (y and z are the directions parallel to the interface) of $<R_g^2>$ and $<R_{ee}^2>$ remain almost unchanged. The variation trend of the mean-square radii of gyration and the three components of the triblock copolymers corresponds well to the chain orientation parameter q. These results can be interpreted as follows: as the chain lengths of homopolymers are

shorter, the triblock copolymers are more stretched in the x-direction, being perpendicular to the interface, and the distribution of the A end block of the triblock copolymers is broader (as illustrated in Figure S5a,b) in the supplementary material, which results in the larger values of q, $<R_g^2>$, $<R_g^2>_x$ and $<R_{ee}^2>_x$ of the triblock copolymers.

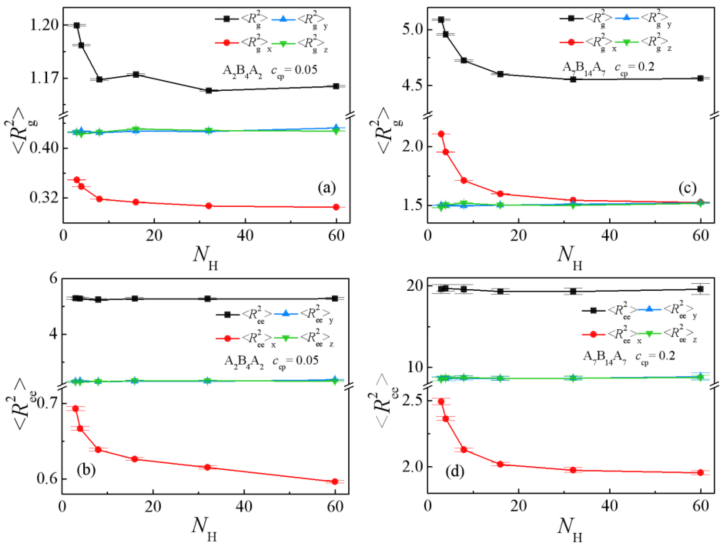

Figure 7. Mean-square radii of gyration $<R_g^2>$ and the three components $<R_g^2>_x$, $<R_g^2>_y$, $<R_g^2>_z$ as a function of the homopolymer chain length with (**a**) $A_2B_4A_2$, c_{cp} = 0.05 (**c**) $A_7B_{14}A_7$, c_{cp} = 0.2. Mean-square end-to-end distance $<R_{ee}^2>$ and the three components $<R_{ee}^2>_x$, $<R_{ee}^2>_y$, $<R_{ee}^2>_z$ as a function of the homopolymer chain length with (**b**) $A_2B_4A_2$, c_{cp} = 0.05 (**d**) $A_7B_{14}A_7$, c_{cp} = 0.2. (N_H = 3, 4, 8, 16, 32, 48, 60).

3.2.2. The Chain Length Effect of Single Homopolymer Component

We further study the dependence of interfacial properties of the $A_n/A_7B_{14}A_7/B_m$ ternary blends on the chain length effect of single homopolymer component. For comparison, we consider the cases with (i) the chain length of polymer A_n fixed as N_{HA} = 4, the chain length of polymer B_m changing from N_{HB} = 4 to N_{HB} = 64, and (ii) N_{HB} = 4 fixed, N_{HA} changing from 4 to 64.

Figure 8a,b show the dependence of the interfacial tension γ and the interfacial width w on the chain length of a single homopolymer component. As can be seen, the interfacial tension γ rapidly increases with increasing N_{HA} and N_{HB} from 4 to 32 at the two blend systems. This finding agrees well with the studies on $A_2/A_2B_8/B_2(B_{10})$ ternary blends of Guo et al. [1]. When N_{HA} and N_{HB} increase from 32 to 60, the interfacial tension γ of the two systems remains almost unchanged, which is shown in Figure 8a. Figure 8b shows the interfacial width w for the two systems. For the case of N_{HA} = 4, the interfacial width w obviously decreases with increasing the homopolymer chain length N_{HB} from 4 to 8, whereas as N_{HB} increases from 8 to 64, the interfacial width w slowly decreases; for the system of N_{HB} = 4, the interfacial width w decreases with increasing of homopolymer chain length N_{HA} from 4 to 16, whereas as N_{HA} increases from 16 to 64, the interfacial width w slowly decreases. This result is because that the shorter the chain length of the homopolymers can cause a wider the interfacial width w (Figure 8b), which results in the decayed correlations between beads of immiscible homopolymers and the smaller interfacial tension γ.

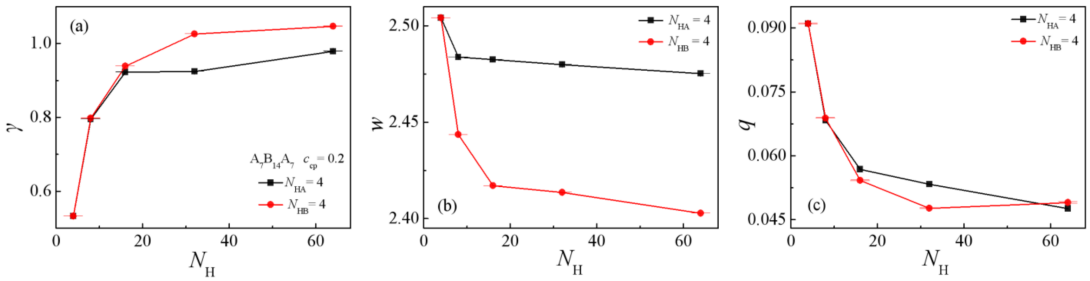

Figure 8. Interfacial tension γ (**a**), interfacial thickness w (**b**), and orientation parameter q of the triblock (**c**) as a function of one kind homopolymer chain length N_H (N_H = 4, 8, 16, 32, 64).

Figures 8c and 9 show the chain orientation parameter q and the dimension of the triblock copolymers on the chain length of a single homopolymer component. The triblock chain orientation parameter q decreases with increasing homopolymer chain length N_{HA} and N_{HB} from 4 to 32, whereas as N_{HA} and N_{HB} further increase from 32 to 64, the q values of the triblock copolymers in both systems change slightly (as illustrated in Figure 8c). Figure 9 depicts the dependence of the dimension of the triblock copolymer on the chain length of a single component homopolymer. For the N_{HA} = 4 system (see the solid line in Figure 9a,b), the $<R_g^2>$ and $<R_g^2>_x$ of the triblock copolymers decrease with increasing homopolymers chain length N_{HB} from 4 to 16, whereas as N_{HB} increases from 16 to 64, the $<R_g^2>$ and $<R_g^2>_x$ remain almost unchanged. For the N_{HB} = 4 system (see the dotted line of Figure 9c,d), the variety of $<R_g^2>$ and the three components are consistent with the N_{HA} = 4 system. Meanwhile, $<R_{ee}^2>_x$ decreases rapidly with the increase of homopolymer chain length N_{HA} from 4 to 32, but as N_{HA} increases from 32 to 64, the $<R_{ee}^2>_x$ almost remains unchanged. This implies that the increase of the homopolymer chain length N_{HA} has a greater impact on the $<R_{ee}^2>_x$, which is directly related to the construction of the triblock copolymer, i.e., the two end blocks of the triblock copolymer composed of A beads. The results can be interpreted as follows: as the chain lengths of homopolymers A_n are shorter and the chain length of homopolymers B_m is fixed to be N_{HB} = 4, the distribution of the A end blocks of the triblock copolymers is broader, as illustrated in Figure S5d, which results in a larger value of $<R_{ee}^2>_x$. By comparing Figure 9a–d with Figure 7c,d, we find that: (1) $<R_g^2>_x$ is always larger than $<R_g^2>_y$ or $<R_g^2>_z$ for the N_{HA} = 4 and N_{HB} = 4 systems, whereas the three components of $<R_g^2>$ are almost the same as the chain length of the homopolymers $N_H > 32$ for the $N_{HA} = N_{HB} = N_H$ systems; (2) for the system with N_{HA} = 4, as N_{HB} increases from 4 to 64, the $<R_{ee}^2>_x$ almost remains unchanged. These results illustrate that the stretch of the triblock copolymers depends on the chain length of the homopolymers, whereas $<R_{ee}^2>_x$ only depends on the chain length of homopolymers N_{HA}, due to the structure of the triblock copolymers. Specifically, the two end blocks (composed of *A* beads) of the triblock copolymers segregate into the homopolymer A_n bulk phase (as illustrated in Figure 1). The increase in chain length of the homopolymer B_m cannot significantly affect the structures of A end blocks of the copolymers, and therefore $<R_{ee}^2>_x$, $<R_{ee}^2>_y$, and $<R_{ee}^2>_z$ almost remain unchanged.

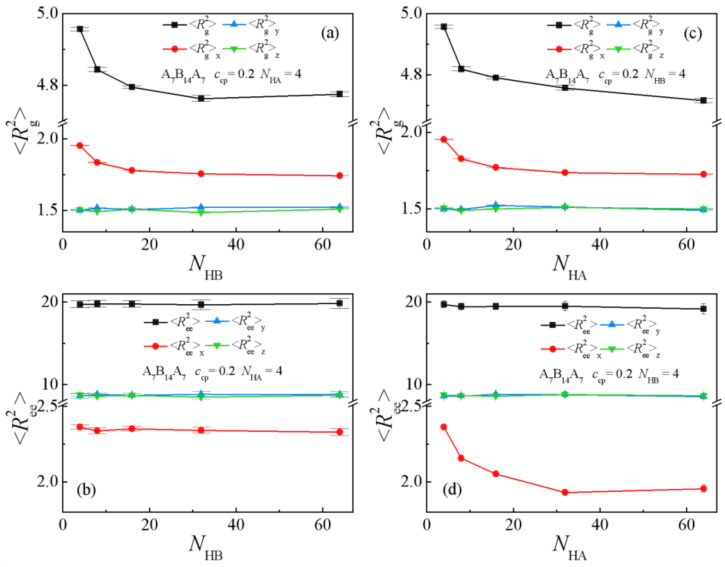

Figure 9. (**a**,**c**) Mean-square radii gyration $<R_g^2>$ and the three components $<R_g^2>_x$, $<R_g^2>_y$, $<R_g^2>_z$, (**b**,**d**) Mean-square end-to-end distance $<R_{ee}^2>$ and the three components $<R_{ee}^2>_x$, $<R_{ee}^2>_y$, $<R_{ee}^2>_z$ as a function of the chain length of single homopolymer component with $A_7B_{14}A_7$, c_{cp} = 0.2. (N_{HA}/N_{HB} = 4, 8, 16, 32, 60).

The interfacial tension γ of the N_{HA} = 4 system (N_{HB} > 16) is less than the N_{HB} = 4 system (N_{HA} > 16); the interfacial width w of the N_{HA} = 4 system (N_{HB} > 16) is larger than the N_{HB} = 4 system (N_{HA} > 16), which results in the correlations between beads A_n and B_m of homopolymers decrease, thus the triblock copolymers compatibilizers show better performance in reducing the interfacial tension of the ternary blends with N_{HA} = 4.

The above analysis clearly shows that for the case of N_{HA} = N_{HB}, N_{HA} = 4, and N_{HB} = 4, as the homopolymer chain length is N_H > 32, the interfacial properties slightly change with the increase of homopolymer chain length. This is because as the chain lengths of the homopolymers are much longer than the corresponding blocks of the triblock copolymers, the homopolymers cannot penetrate the copolymers blocks layer [20], and therefore the increase of the homopolymers chain length slightly affect the interfacial properties.

4. Conclusions

In this paper, we investigated the effects of the repulsion parameter and chain length of the homopolymers on the interfacial properties of ternary $A_n/A_{x/2}B_xA_{x/2}/B_m$ polymeric blends using dissipative particle dynamics (DPD) simulations.

By comparing the interfacial tension and the density distribution of the triblock copolymers of the $A_8/A_2B_4A_2/B_8$ and $A_8/A_7B_{14}A_7/B_8$ blends at different repulsion parameters, we find that at a repulsion parameter (a_{AB} = 40), the ternary blends exhibit the maximum segregation with lower interfacial tension and stronger adhesion.

We then compare the efficiency of the triblock copolymer on stabilizing the blends of incompatible homopolymers at different chain lengths. For the case of chain lengths of homopolymers N_{HA} = N_{HB}, both the interfacial tension and the density of triblock copolymer at the center of the interface increase to a plateau with increasing the homopolymer chain length, which indicates that the triblock copolymers exhibit better performance as the compatibilizers for blending homopolymers with shorter chain length due to the more stretched conformations of triblock copolymers. For the case of fixing one homopolymer chain length system (the system with N_{HA} = 4 or the system with N_{HB} = 4), the triblock copolymers ($A_{x/2}B_xA_{x/2}$) compatibilizers show better performance in reducing the interfacial tension for blends with N_{HA} = 4, compared to the blends with N_{HB} = 4.

Our simulations indicate that the interfacial properties of the ternary $A_n/A_{x/2}B_xA_{x/2}/B_m$ polymeric blends are strongly correlated to repulsion parameters and the chain length of the incompatible homopolymers, which provides insights into the fundamental understanding of the interfacial properties of polymer blends. In this context, it would also be interesting to systematically study the influence of other physical factors on the interfacial properties of the polymeric blend at the microscopic level. In addition, with the development of polymer synthesis technology, ionic polymer blends have attracted extensive attention as new materials due to their ideal ionic conductivity and mechanical strength [46]. We predict that adding block copolymers (as a compatibilizer) into the ionic polymeric blends might modify the physicochemical property of the polymer electrolytes.

Supplementary Materials: The following are available online at https://www.mdpi.com/article/10.3390/polym13142333/s1, Figure S1: (a) R_g^2 and (b) R_{ee}^2 of the triblock copolymers for the case $A_8/A_2B_4A_2/B_8$ with c_{cp}=0.05 as a function of the simulation time; (c) R_g^2 and (d) R_{ee}^2 of the triblock copolymers for the case $A_8/A_7B_{14}A_7/B_8$ with c_{cp} = 0.2 as a function of the simulation time. Figure S2: (a) Representative snapshots of the "hairpin" structure for $A_7B_{14}A_7$. (b) Morphology snapshot of the copolymers for $A_2B_4A_2$, c_{cp} = 0.05, a_{AB} = 30. The red and yellow spheres denote bead A and bead B of homopolymers A_8 and B_8, and the green and blue spheres represent beads A and B of the triblock. Figure S3: Morphology snapshots for ternary mixtures $A_8/A_2B_4A_2/B_8$, c_{cp} = 0.2, a_{AB} = 40. The red and yellow spheres denote bead A and bead B of homopolymers, and the green and blue spheres represent beads A and B of the triblock., Figure S4: Density profiles of beads A, B of the triblock copolymer along the *x*-axis as a function of the repulsion parameter a_{AB} with (a) $A_2B_4A_2$, c_{cp} = 0.05 and (b) $A_7B_{14}A_7$, c_{cp} = 0.2. Figure S5: Density profiles of beads A, B of the triblock copolymer along the *x*-axis as a function of chain length of the homopolymers $N_H = N_{HA} = N_{HB}$ with (a) $A_2B_4A_2$, c_{cp} = 0.05, (b) $A_7B_{14}A_7$, c_{cp} = 0.2. Density profiles of beads A, B of the triblock copolymer along the *x*-axis as a function of one homopolymers chain length with (c) $A_7B_{14}A_7$, c_{cp} = 0.2, N_{HA} = 4 (d) $A_7B_{14}A_7$, c_{cp} = 0.2, N_{HA} = 4.

Author Contributions: Conceptualization, D.L. and X.D.; methodology, D.L., X.D. and T.L.; validation, D.L. and X.D.; formal analysis, D.L. and X.D.; resources, Y.L. and K.G.; data curation, Y.L.; writing—original draft preparation, D.L.; writing—review and editing, D.L., X.D. and H.B.; supervision, D.L., T.L. and X.D.; project administration, D.L., K.G., T.L., X.D. and H.B.; funding acquisition, D.L. and X.D. All authors have read and agreed to the published version of the manuscript.

Funding: This research was funded by the Basic Scientific Research Project of Hebei Provincial Department of Education (grant JQN2020021), the National Natural Science Foundation of China (grant 22073094), the Science and Technology Development Program of Jilin Province (grant 202523GH010572817) of China, the State Key Laboratory of Molecular Engineering of Polymers (Fudan University) (grant K2020-13 and K2021-01) and the Natural Science Foundation of Hebei Province (Nos. A2018209147).

Institutional Review Board Statement: Not applicable.

Informed Consent Statement: Not applicable.

Data Availability Statement: Data is contained within the article or supplementary material.

Acknowledgments: This work is financially supported by the Basic Scientific Research Project of Hebei Provincial Department of Education (grant JQN2020021), the National Natural Science Foundation of China (grant 22073094), the Science and Technology Development Program of Jilin Province (grant 202523GH010572817) of China, the State Key Laboratory of Molecular Engineering of Polymers (Fudan University) (grant K2020-13 and K2021-01) and the Natural Science Foundation of Hebei Province (Nos. A2018209147). We are grateful for the essential supports of Hebei Key Laboratory of Data Science and Application.

Conflicts of Interest: The authors declare no conflict of interest.

References

1. Guo, H.X.; Cruz, M.O. A computer simulation study of the segregation of amphiphiles in binary immiscible matrices: Short asymmetric copolymers in short homopolymers. *J. Chem. Phys.* **2005**, *123*, 174903. [CrossRef]
2. Anastasiadis, S.H. Interfacial tension in binary polymer blends and the effects of copolymers as emulsifying agents. *Adv. Polym. Sci.* **2011**, *238*, 179–269.

3. Yu, Q.Y.; Zhang, C.L.; Gu, X.P.; Wang, J.J.; Feng, L.F. Compatibilizing efficiency of copolymer precursors for immiscible polymer blends. *J. Appl. Poly. Sci.* **2012**, *124*, 3392–3398. [CrossRef]
4. Chang, K.; Macosko, C.W.; Morse, D.C. Ultralow interfacial tensions of polymer/polymer interfaces with diblock copolymer surfactants. *Macromolecules* **2007**, *40*, 3819–3830. [CrossRef]
5. Retsos, H.; Margiolaki, A.; Anastasiadis, S.H. Interfacial tension in binary polymer blends in the presence of block copolymers: Effects of additive MW. *Macromolecules* **2001**, *34*, 5295–5305. [CrossRef]
6. Retsos, H.; Anastasiadis, S.H.; Pispas, S.; Mays, J.W.; Hadjichristidis, N. Interfacial tension in binary polymer blends in the presence of block copolymers. 2. effects of additive architecture and composition. *Macromolecules* **2004**, *37*, 524–537. [CrossRef]
7. Zhou, Y.X.; Huang, M.X.; Lu, T.; Guo, H.X. Nanorods with different surface properties in directing the compatibilization behavior and the morphological transition of immiscible polymer blends in both shear and shear-free conditions. *Macromolecules* **2018**, *51*, 3135–3148. [CrossRef]
8. Qian, H.J.; Lu, Z.Y.; Chen, L.J.; Li, Z.S.; Sun, C.C. Dissipative particle dynamics study on the interfaces in incompatible A/B homopolymer blends and with their block copolymers. *J. Chem. Phys.* **2005**, *122*, 187907. [CrossRef]
9. Lemos, T.; Abreu, C.; Pinto, J.C. DPD simulations of homopolymer-copolymer-homopolymer mixtures: Effects of copolymer structure and concentration. *Macromol. Theory Simul.* **2020**, *29*, 2000014. [CrossRef]
10. Balazs, A.C.; Siemasko, C.P.; Lantman, C.W. Monte-Carlo simulations for the behavior of multiblock copolymers at a penetrable interface. *J. Chem. Phys.* **1991**, *94*, 1653–1663. [CrossRef]
11. Wang, Y.M.; Mattice, W.L. Simulation of the adsorption of symmetric diblock copolymers at the interface of the two monomeric homopolymers. *J. Chem. Phys.* **1993**, *98*, 9881–9887. [CrossRef]
12. Wang, Y.M.; Mattice, W.L. Simulation of the adsorption of unsymmetric diblock copolymers at the interface between the two monomeric homopolymers. *J. Chem. Phys.* **1993**, *99*, 4068–4075. [CrossRef]
13. Schmid, F.; Müller, M. Quantitative comparison of self-consistent-field theories for polymers near interfaces with monte-carlo simulations. *Macromolecules* **1995**, *28*, 8639–8645. [CrossRef]
14. Müller, M.; Schick, M. Bulk and interfacial thermodynamics of a symmetric, ternary homopolymer-copolymer mixture: A Monte Carlo study. *J. Chem. Phys.* **1996**, *105*, 8885–8901. [CrossRef]
15. Werner, A.; Schmid, F.; Binder, K.; Müller, M. Diblock copolymers at a homopolymer-homopolymer interface: A Monte Carlo simulation. *Macromolecules* **1996**, *29*, 8241–8248. [CrossRef]
16. Liu, D.M.; Duan, X.Z.; Shi, T.F.; Jiang, F.; Zhang, H.Z. Monte carlo simulation of effects of homopolymer chain length on interfacial properties of A/AB/B ternary polymer blends. *Chem. J. Chin. Univ. Chin.* **2015**, *36*, 2532–2539.
17. Liu, D.M.; Dai, L.J.; Duan, X.Z.; Shi, T.F.; Zhang, H.Z. Monte Carlo Simulation of Interfacial Properties in Homopolymer/Diblock Copolymer/Homopolymer Ternary Polymer Blends. *Chem. J. chin. Univ. Chin.* **2015**, *36*, 1752–1758.
18. Wanakule, N.S.; Nedoma, A.J.; Robertson, M.L.; Fang, Z.; Jackson, A.; Garetz, B.A.; Balsara, N.P. Characterization of micron-sized periodic structures in multicomponent polymer blends by ultra-small-angle neutron scattering and optical microscopo. *Macromolecules* **2008**, *41*, 471–477. [CrossRef]
19. Garnier, S.; Laschewsky, A. New amphiphilic diblock copolymers: Surfactant properties and solubilization in their micelles. *Langmuir* **2006**, *22*, 4044–4053. [CrossRef]
20. Fortelny, L.; Juza, J. Analysis of the effect of block copolymers on interfacial tension in immiscible polymer blends. *Polymer* **2018**, *150*, 380–390. [CrossRef]
21. Goodson, A.D.; Liu, G.L.; Rick, M.S.; Raymond, A.W.; Uddin, M.F.; Ashbaugh, H.S.; Albert, J.N.L. Nanostructure stability and swelling of ternary block copolymer/homopolymer blends: A direct comparison between dissipative particle dynamics and experiment. *J. Polym. Sci. Pt. B Polym. Phys.* **2019**, *57*, 794–803. [CrossRef]
22. Russell, T.P.; Mayes, A.M.; Deline, V.R.; Chung, T.C. Hairpin configurations of triblock copolymers at homopolymer interfaces. *Macromolecules* **1992**, *25*, 5783–5789. [CrossRef]
23. Dai, K.D.; Washiyama, J.; Kramer, E.J. Segregation study of a BAB triblock copolymer at the A/B homopolymer interface. *Macromolecules* **1994**, *27*, 4544–4553. [CrossRef]
24. Wagner, M.; Wolf, B.A. Effect of block copolymers on the interfacial-tension between 2. Immiscible/homopolymers. *Polymer* **1993**, *34*, 1460–1464. [CrossRef]
25. Jorzik, U.; Wagner, M.; Wolf, B.A. Effect of block copolymer architecture on the interfacial tension between immiscible polymers. *Prog. Colloid. Polym. Sci.* **1996**, *101*, 170–171.
26. Xu, Y.; Thurber, C.M.; Macosko, C.W.; Lodge, T.P.; Hillmyer, M.A. Poly(methyl methacrylate) -block -polyethylene -block -poly(methyl methacrylate) Triblock Copolymers as Compatibilizers for Polyethylene/Poly(methyl methacrylate) Blends. *Ind. Eng. Chem. Res.* **2014**, *53*, 4718–4725. [CrossRef]
27. Sun, Z.Q.; Zhang, B.; Bian, X.C. Synergistic effect of PLA-PBAT-PLA tri-block copolymers with two molecular weights as compatibilizers on the mechanical and rheological properties of PLA/PBAT blends. *RSC Adv.* **2015**, *5*, 73842–73849. [CrossRef]
28. Zhao, X.Y.; Huang, Y.J.; Kong, M.Q.; Li, G.X. Assessment of compatibilization efficiency of SEBS in the PP/PS blend. *J. Appl. Polym. Sci.* **2018**, *135*, 46244. [CrossRef]
29. Liu, D.M.; Gong, K.; Lin, Y.; Liu, T.; Liu, Y.; Duan, X.Z. Dissipative Particle Dynamics Study on Interfacial Properties of Symmetric Ternary Polymeric Blends. *Polymers.* **2021**, *13*, 1516. [CrossRef]

30. Zhu, P.F.; Li, Y.; Li, Q.W. Mesoscopic simulation of the interfacial behavior of biosurfactant rhamnolipids and the synergistic systems. *Acta. Chim. Sin.* **2011**, *69*, 2420–2426.
31. Catarino, C.R.; Bustamante-Rendon, R.A.; Hernandez–Fragoso, J.S. Surfactant chain length and concentration influence on the interfacial tension of two immiscible model liquids: A coarse-grained approach. *J. Mol. Model.* **2017**, *23*, 306. [CrossRef]
32. Zhang, Y.Z.; Xu, J.B.; He, X.F. Effect of surfactants on the deformation of single droplet in shear flow studied by dissipative particle dynamics. *Mol. Phys.* **2018**, *116*, 1851–1861. [CrossRef]
33. Liang, X.P.; Wu, J.Q.; Yang, X.G. Investigation of oil-in-water emulsion stability with relevant interfacial characteristics simulated by dissipative particle dynamics. Colloid surf. A-Physicochem. *Eng. Asp.* **2018**, *546*, 107–114. [CrossRef]
34. Wang, S.Y.; Yang, S.W.; Wang, R.C. Dissipative particle dynamics study on the temperature dependent interfacial tension in surfactant-oil-water mixtures. *J. Pet. Sci. Eng.* **2018**, *169*, 81–95. [CrossRef]
35. Goodarzi, F.; Zendehboudi, S. Effects of salt and surfactant on interfacial characteristics of water/oil systems: Molecular dynamic simulations and dissipative particle dynamics. *Ind. Eng. Chem. Res.* **2019**, *58*, 8817–8834. [CrossRef]
36. Goodarzi, F.; Kondori, J.; Rezaei, N. Meso- and molecular-scale modeling to provide new insights into interfacial and structural properties of hydrocarbon/water/surfactant systems. *J. Mol. Liq.* **2019**, *295*, 111357. [CrossRef]
37. Li, B.Y.; Zhao, L.; Lu, Z.Y. Microscopic characteristics of janus nanoparticles prepared via a grafting-from reaction at the immiscible liquid interface. *Phys. Chem. Chem. Phys.* **2020**, *22*, 5347–5354. [CrossRef]
38. Schlijper, A.G.; Hoogerbrugge, P.J.; Manke, C.W. Computer-simulation of dilute polymer-solutions with the dissipative particle dynamics method. *J. Rheol.* **1995**, *39*, 567–579. [CrossRef]
39. Lin, Y.; Boker, A.; He, J.; Sill, K.; Xiang, H.; Abetz, C.; Li, X.; Wang, J.; Emrick, T.; Long, S.; et al. Self-directed self-assembly of nanoparticle/copolymer mixtures. *Nature* **2005**, *434*, 55–59. [CrossRef]
40. Hong, Z.H.; Xiao, N.; Li, L.; Xie, X.N. Investigation of nanoemulsion interfacial properties: A mesoscopic simulation. *J. Food Eng.* **2020**, *276*, 109877. [CrossRef]
41. Zhang, J.W.; Chen, L.; Wang, A.L.; Yan, Z.C. Dissipative particle dynamics simulation of ionic liquid-based microemulsion: Quantitative properties and emulsification mechanism. *Ind. Eng. Chem. Res.* **2020**, *59*, 763–773. [CrossRef]
42. Groot, R.D.; Warren, P.B. Dissipative particle dynamics: Bridging the gap between atomistic and mesoscopic simulation. *J. Chem. Phys.* **1997**, *107*, 4423–4435. [CrossRef]
43. Zhou, Y.; Long, X.P.; Zeng, Q.X. Simulation studies of the interfaces of incompatible glycidyl azide polymer/hydroxyl-terminated polybutadiene blends by dissipative particle dynamics. I. The effect of block copolymers and plasticizers. *J. Appl. Poly. Sci.* **2012**, *125*, 1530–1537. [CrossRef]
44. Irving, J.H.; Kirkwood, J.G. The statistical mechanical theory of transport processes.4. the equations of hydrodynamics. *J. Chem. Phys.* **1950**, *18*, 817–829. [CrossRef]
45. Helfand, E.; Tagami, Y. Theory of the Interface Between Immiscible Polymers. *J. Chem. Phys.* **1972**, *57*, 3592–3601. [CrossRef]
46. Liu, B.L.; Hu, B.; Du, J.; Cheng, D.M.; Zang, H.Y.; Ge, X.; Tan, H.Q.; Wang, Y.H.; Duan, X.Z.; Jin, Z.; et al. Precise Molecular-Level Modification of Nafion with Bismuth Oxide Clusters for High-performance Proton-Exchange Membranes. *Angew. Chem. Int. Edit.* **2021**, *60*, 6076–6085. [CrossRef] [PubMed]